Semat, H., *Introduction to Atomic and Nuclear Physics*, Rinehart & Co., Inc., New York (1958).
Weinstein, J., and R. J. Adler, "Micromixing Effects in Continuous Chemical Reactors," *Chem. Eng. Sci.*, **22**, p. 65 (1967).

NOTATION

A = activity of radionuclide tracer
B_{ij} = fraction of fluid in subcompartment i that derives from substream j
C = concentration
E = gamma ray energy
h = enthalpy
Q = flow rate
R = residual tracer activity
t = time
V = volume
w = mass rate of tracer flow
W = total tracer mass
α = counting efficiency constant
θ = angle of gamma ray scatter

Subscripts

E = equilibrium
i = subcompartment designator
j = flow stream designator
T = total system

Manuscript received October 30, 1981; revision received April 15 and accepted April 29, 1983.

Hydrodynamics and Mass Transfer in Non-Newtonian Solutions in a Bubble Column

Until now the oxygen transfer in viscous non-Newtonian solutions has been studied only in bubble columns of about 0.14-m diameter. Recently Godbole et al. (1982) reported much smaller gas holdups in Carboxy Methyl Cellulose solutions (CMC) for a large-diameter column. Therefore, the gas holdups, volumetric mass transfer coefficients, and specific gas-liquid interfacial areas are measured in CMC solutions using a bubble column of diameter 0.305 m and height 3.4 m. The transition from churn-turbulent to slug flow regime occured at higher viscosities and the gas holdups and volumetric mass transfer coefficients were lower in both flow regimes than reported for smaller column diameters. Empirical correlations are presented for the gas holdup, volumetric mass transfer coefficient, and specific gas-liquid interfacial area which would be suitable for the design of fermentors.

S. P. GODBOLE, A. SCHUMPE, and Y. T. SHAH

Chemical and Petroleum Engineering Department
University of Pittsburgh
Pittsburgh, PA 15261
and

N. L. CARR

Gulf Research and Development Co.
Harmerville, Pittsburgh, PA 15230

SCOPE

Bubble column reactors are becoming increasingly popular in the biotechnological and pharmaceutical industry. The rheological behavior of microbiological cultures in a fermentation tower can be fairly well simulated by the solutions of carboxymethyl cellulose (CMC). All the literature data for the hydrodynamics and mass transfer in CMC solutions were taken in columns of up to 0.14-m diameter. Recently for viscous CMC solutions, Godbole et al. (1982) reported a strong decrease in the gas holdup with an increase in the column diameter. The strong dependency of the gas holdup on column diameter suggests a similar dependency for the volumetric mass transfer coefficient, i.e., the previous investigations in columns of 0.14-m diameter are insufficient for scale-up purposes. The correlation of Nakanoh and Yoshida (1980) even suggests an increase in volumetric mass transfer coefficient with increasing column diameter. Therefore, in this work oxygen mass transfer in CMC solution was studied in a 0.305-m diameter column.

Volumetric mass transfer coefficients are measured by the dynamic method. Specific interfacial areas are determined by the sulfite oxidation technique used by Schumpe and Deckwer (1982). The kinetics of the cobalt catalyzed reaction is not affected by addition of CMC (Wesselingh and van't Hoog, 1970); Onken and Schalk, 1978; Poggemann, 1982) and the deviation of the chemically effective interfacial area from the geometrical one is small because of the small gas-phase conversion (Schumpe and Deckwer, 1980a,b). The gas holdups are measured using a hydrostatic head technique and fractional gas holdups are measured using the dynamic gas disengagement technique (Sriram and Mann, 1976). To study the influence of the added salt, volumetric mass transfer coefficients are determined in CMC/sodium sulfate solutions and compared with the k_La values obtained in pure CMC solutions. Fermentation media might be more complex than the model media used and hence the effect of surfactant (Triton X-114) on the hydrodynamics and mass transfer in CMC solutions is studied. The gas holdup, volumetric mass transfer coefficient, and gas-liquid interfacial area are correlated empirically. These correlations are based on data collected in a large-diameter column for wide ranges of gas throughputs and apparent liquid-phase viscosities and hence would be better suited for the scale-up of fermentors than those presently available.

A. Schumpe is currently with the Techn. Chemie, FB 9, Univ. Oldenburg, Oldenburg, W. Germany.

CONCLUSIONS AND SIGNIFICANCE

The bubble sizes observed in viscous solutions suggest that the effect of column diameter on ϵ_G, a, k_La, etc. would prevail up to larger diameters for viscous solutions than for low-viscosity solutions. Hydrodynamics and mass transfer in highly viscous pseudoplastic solutions have been studied in bubble columns of diameters up to 0.14 m. Therefore, the hydrodynamic and mass transfer data for viscous pseudoplastic solutions in a large-diameter column (0.305 m) over a wide range of gas velocities would be useful for scale-up purposes.

Transition from churn-turbulent to slug flow occurred at a viscosity of 0.1 Pa·s as compared to 0.02–0.03 Pa·s in 0.14-m diameter columns. For the churn-turbulent flow regime, correlations for gas holdup, gas-liquid interfacial areas, and volumetric mass transfer coefficients were developed:

$$\epsilon_G = 0.207\ V_G^{0.6}\ \mu_{\text{eff}}^{-0.19} \qquad (\text{ms}^{-1}\ \text{Pa·s})$$

$$k_La = 8.35 \times 10^{-4}\ V_G^{0.44}\ \mu_{\text{eff}}^{-1.01} \qquad (\text{s}^{-1};\ \text{ms}^{-1}\ \text{Pa·s})$$

$$a = 19.2\ V_G^{0.47}\ \mu_{\text{eff}}^{-0.76} \qquad (\text{m}^{-1};\ \text{ms}^{-1}\ \text{Pa·s})$$

All the three parameters (ϵ_G, k_La and a) show a stronger dependency on viscosity than corresponding relations for the slug flow regime. Because of the strong influence of column diameter, further investigations in a larger bubble column might be required for reliable scale-up.

In the churn-turbulent flow regime, addition of 0.8 mol·L^{-1} sodium sulfate or sulfite increased the gas holdups by 23% and the volumetric mass transfer coefficients increased by a factor of 2.5. It further retarded the transition of slug flow to higher viscosities (around 0.2 Pa·s). The gas-liquid interfacial areas measured by sulfite oxidation could be applied only to volumetric mass transfer coefficients in equimolar CMC/sodium sulfate solutions. The resulting liquid-side mass transfer coefficients k_L were almost independent of superficial gas velocity and decreased slightly with apparent liquid-phase viscosity.

Addition of surfactants increased the gas holdup exclusively by increasing the gas holdup of very small bubbles ($d_B < 1$ mm). The k_La values increased strongly with decreasing surface tension. The determined dependency ($k_La\ \alpha\ \sigma^{-1.25}$) may be treated as an upper limit. The presence of salts and surfactants are common for microbial culture media which is simulated by the highly viscous pseudoplastic solutions. Therefore, the present results for such additives to highly viscous CMC solutions are of importance for the application of correlations developed for CMC model media to the fermentation process.

INTRODUCTION

Hydrodynamics and mass transfer in non-Newtonian solutions are so far studied in small diameter bubble columns. The hydrodynamics and mass transfer in pseudoplastic solutions of CMC in bubble columns (D_c = 0.14 m) were first studied by Buchholz et al. (1978) and Voigt et al. (1980). These investigations were summarized by Schugerl (1981) and the results were correlated by Henzler (1980). The mass transfer coefficients were much higher than those recently reported by Nakanoh and Yoshida (1980) and Deckwer et al. (1982).

Nakanoh and Yoshida (1980) determined volumetric mass transfer coefficients in solutions of sucrose, CMC and sodium polyacrylate. The measurements were carried out by the dynamic method in a bubble column of 0.1445-m diameter. The volumetric mass transfer coefficients were correlated by

$$\frac{k_La'}{D_L} D_C = 0.09 Sc^{0.5} Bd^{0.75} Ga^{0.39} Fr^{1.00} (1 + cDe^m)^{-1} \qquad (1)$$

Equation 1 was obtained from the correlation of Akita and Yoshida (1974) by a mere adjustment of the constant factor to fit the data. For solutions with negligible elastic properties, Eq. 1 can be written as

$$k_La' = 0.09 V_G^{1.00} \mu_{\text{eff}}^{-0.28} D_c^{0.17} D_L^{0.5} \sigma^{-0.75} \rho^{1.03} g^{0.64} \qquad (2)$$

Deckwer et al. (1982) pointed out that the proportionality of k_La' to superficial gas velocity is uncommon for churn-turbulent flow. Their own measurements were carried out in a 0.14-m diameter column. The volumetric mass transfer coefficients were obtained by application of the axial dispersion model to profiles of the liquid-phase oxygen concentration measured under stationary conditions. At low gas velocities, the mass transfer coefficients were strongly dependent on the type of gas distributor used. At gas velocities higher than 0.02 ms^{-1} and apparent liquid viscosities above 0.02–0.03 Pa·s, gas slugs were formed and for all applied gas spargers the volumetric mass transfer coefficients k_La (with respect to dispersion volume) were correlated by:

$$k_La = 3.15 \times 10^{-3}\ V_G^{0.59}\ \mu_{\text{eff}}^{-0.84} \qquad (\text{s}^{-1};\ \text{ms}^{-1}\ \text{Pa·s}) \qquad (3)$$

For calculation of effective liquid-phase viscosity μ_{eff}, Nakanoh and Yoshida (1980) and Deckwer et al. (1982) applied a relation for shear rate γ proposed by Nishikawa et al. (1977).

$$\gamma = 5{,}000\ V_G \qquad (\text{s}^{-1};\ \text{ms}^{-1}) \qquad (4)$$

In the bubble column used by Deckwer et al. (1982), Schumpe and Deckwer (1982) measured specific interfacial areas in CMC solutions by the sulfite oxidation technique. In the slug flow regime, there was no effect of addition of sodium sulfite (0.8 mol·L^{-1}) on gas holdups and bubble frequencies. Volumetric mass transfer coefficients in a CMC solution containing 0.8 mol·L^{-1} sodium sulfate were well described by Eq. 3. For the gas-liquid interfacial areas in the slug flow regime the following relation was suggested

$$a = 48.7\ V_G^{0.51}\ \mu_{\text{eff}}^{-0.51} \qquad (\text{m}^{-1};\ \text{ms}^{-1}\ \text{Pa·s}) \qquad (5)$$

The liquid-side mass transfer coefficients (k_L) resulting from the application of Eq. 5 to the k_La data were almost independent of the gas velocity. (For the CMC/sodium sulfate solution they were about 1.3×10^{-4} ms^{-1}.)

Poggemann (1982) also applied the sulfite oxidation technique to measure gas-liquid interfacial areas in CMC solutions in a bubble column with a two-phase nozzle. However, in this reactor mass transfer occurred in the impulse exchange tube rather than the bubble column zone.

All the previous mass transfer measurements were carried out in bubble columns of almost the same diameter (0.14–0.1455 m). Gas holdups were also measured in a 0.102-m diameter column by Schumpe and Deckwer (1982), who observed higher gas holdups for the smaller column diameter. In the churn turbulent flow regime the gas holdups decreased with increasing viscosity until gas slugs were formed at a viscosity of about 0.02–0.03 Pa·s. In the slug flow regime the gas holdups were independent of liquid-phase viscosity. For 0.102-m and 0.14-m diameter columns the gas holdups were correlated by Eqs. 6 and 7 respectively

$$\epsilon_G = 0.725\ V_G^{0.627} \qquad (\text{ms}^{-1}) \qquad (6)$$

and

$$\epsilon_G = 0.718\, V_G^{0.674} \quad \text{ms}^{-1} \tag{7}$$

Recently Godbole et al. (1982) measured the gas holdups in a 0.305-m diameter column. Even at high viscosities (0.1 Pa·s) the flow was churn-turbulent and (after passing through a maximum around 0.003 Pa·s) the gas holdups decreased with increasing viscosity. They were much smaller than the gas holdup data reported in the literature for smaller diameter columns. On the basis of their own data at high viscosity and the correlations (Eqs. 6 and 7) of Schumpe and Deckwer (1982) for slug flow, they suggested the following diameter dependency.

$$\epsilon_G = 0.239\, V_G^{0.634}\, D_c^{-0.50} \quad \text{ms}^{-1}\ \text{m} \tag{8}$$

Because of such strong dependency of the gas holdups on the column diameter the previous studies of hydrodynamics and mass transfer in pseudoplastic solutions in small diameter columns seem inadequate for scale-up purposes. Therefore, hydrodynamics and mass transfer in highly pseudoplastic CMC solutions were studied in a large-diameter column (D_c = 0.305 m). The gas holdups (hydrostatic head technique), volumetric mass transfer coefficients (dynamic method), and gas-liquid interfacial areas (sulfite oxidation technique) were measured.

Aqueous solutions of CMC are often used to simulate the viscous pseudoplastic media encountered in biotechnological and pharmaceutical processes. However, fermentation media are more complex than the pure CMC solutions as they contain electrolytes and surface-active substances. Hence the effects of salt and surfactant on the gas holdup and mass transfer in CMC solutions are also studied. The presence of surface-active substances in CMC solutions used by Buchholz et al. (1978) and Voigt et al. (1980) might have been the cause of low surface tensions and the presence of many small (d_B < 1 mm) bubbles (Franz et al., 1980). Therefore, in one run a surfactant (Triton X-114: provided by Rohm and Haas) was added to decrease the surface tension. In addition to the influence of surfactant on k_La, the gas holdup structure was investigated using the dynamic gas disengagement technique.

EXPERIMENTAL

The measurements were carried out in a bubble column of 0.305-m diameter and a height of 3.4 m. The gas was distributed by a perforated plate with 749 holes of 1.66-mm diameter. Figure 1 shows a schematic diagram of the experimental setup.

Gas holdups were determined by the manometric method from the difference in hydrostatic head at 0.46-m and 1.98-m height. The holdups were found to be axially independent (Godbole et al., 1982). For determination of the holdup of very small bubbles, aeration of a liquid batch was stopped by closing a magnetic valve and the decrease in dispersion height was recorded.

Volumetric mass transfer coefficients were determined by the dynamic method at a dispersion height of about 2.5 m. For this purpose the liquid was deaerated by sparging nitrogen. After disengagement of the nitrogen bubbles, the air flow was started, and the increase in liquid-phase oxygen concentration measured with an oxygen electrode (Beckmann, Fieldlab oxygen analyzer) was recorded. The electrode was inserted horizontally at a height of 1.52 m by about 0.05 m. Errors due to sticking of bubbles to the membrane were found to be negligible for this arrangement. The first-order time constant was about 4.7 s in water and increased up to three times in CMC solutions.

In presence of surfactant the occurrence of very small bubbles required a modification of the experimental procedure. After deaeration, the complete disengagement of very small nitrogen bubbles required long time (>1 h). During aeration, the formation of very small new bubbles resulted in nonstationary holdups and interfacial areas. Therefore, only the disengagement of the large nitrogen bubbles was waited for and the influence of very small bubbles was corrected for in the reactor model.

During the sulfite oxidation runs the superficial liquid velocity was about 0.006 ms^{-1}. At 2.62-m dispersion height the solution was withdrawn from the column into a stirred storage tank that was equipped with cooling coils. From the tank it was pumped back into the column through an opening in the center of the gas sparger plate. The interfacial area determinations

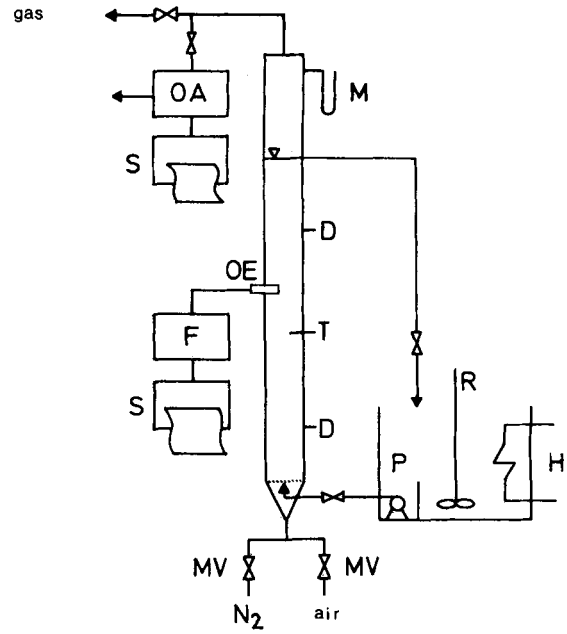

D	Tap for gas holdup measurement	OE	Oxygen Electrode
F	Fieldlab oxygen analyser	P	Pump
H	Cooling coil	R	Rotor
M	Manometer	S	Chart Recorder
MV	Magnetic Valve	T	Thermocouple
OA	Paramagnetic O_2-Analyser		

Figure 1. Experimental setup.

were carried out at pH values of 8.4–8.1 and concentrations of 0.8 mol·L^{-1} sodium sulfite and 8×10^{-4} mol·L^{-1} cobalt sulfate. During the absorption runs the sulfite concentration never decreased below 0.4 mol·L^{-1}. Under these conditions the reaction is second order in oxygen and zero order in sulfite (Linek and Vacek, 1981).

The quasistationary oxygen outlet concentrations were measured by using a paramagnetic oxygen analyser (Beckmann). The actual values of the absorption parameter K_2

$$K_2 = \left(\frac{2k_2D_L}{3H^3}\right)^{0.5} \tag{9}$$

were determined for each run by absorption measurements in a stirred cell with a flat liquid interface.

Liquid-Phase Properties

The CMC solutions were prepared by dissolving CMC powder (7H4 and 7M2, Hercules Inc.) in tap water. The CMC/salt solutions were prepared by combining higher concentrated solutions of the components.

Surface tensions were measured with a Fischer Surface Tensiomat 21. The flow behavior was studied with a concentric cylinder viscometer (Fann, VG-Meter) at shear rates of 5.1–1,022 s^{-1}. This closely corresponds to the range of shear rates encountered in a bubble column at the applied gas velocities of 0.03–0.25 ms^{-1} (Eq. 4). The flow behavior of the pseudoplastic solutions was characterized by the power law model of Ostwald-de Waele as:

$$\Gamma = k\dot{\gamma}^n \tag{10}$$

and

$$\mu_{\text{eff}} = k\dot{\gamma}^{n-1} \tag{11}$$

Table 1 summarizes the fluid consistency indices k, the flow behavior indices n, the equilibrium surface tensions, and the densities of the solutions. The CMC/sulfite solutions encountered a slow viscosity decrease. The actual rheological properties were determined individually for each measurement. The oxygen solubilities were calculated from an empirical model (Schumpe et al., 1982).

Analysis

For evaluation of k_La values from the dynamic absorption runs the same procedure was applied as used by Nakanoh and Yoshida (1980). Complete mixing of the liquid phase was assumed; oxygen depletion in the gas phase could be neglected. The liquid-phase mass balance

$$\frac{dC}{dt} = k_La'(C^* - C) \tag{12}$$

TABLE 1. LIQUID-PHASE PROPERTIES AT 25°C

Solution	n	k Pa·s^n	ρ_L kg·m^{-3}	$10^3\sigma$ N·m^{-1}
CMC Solutions				
1	0.697	0.095	1,000	73.0
2	0.654	0.184	1,000	72.5
3	0.668	0.256	1,002	73.2
4	0.607	0.526	1,003	68.4
5	0.492	2.816	1,005	67.7
6	0.498	4.337	1,006	67.6
7	0.440	7.683	1,006	67.6
CMC/Triton X-114 (0–5.5 × 10^{-5}m) Solution				
1-6	0.627–0.6047	0.373–0.301	1,002	73.6–41.9
CMC/Sodium Sulfate (0.8M) Solution				
1	0.742	0.263	1,008	73.4
2	0.671	0.671	1,101	73.4
3	0.603	1.997	1,101	72.7
CMC/Sodium Sulfite (0.8M) Solution				
1	0.844–0.847	0.068–0.044	1,092	74.6
2	0.698–0.794	0.375–0.144	1,093	74.5
3	0.568–0.654	1.563–0.739	1,094	74.5
4	0.482–0.522	4.824–3.533	1,096	74.6

and a first-order time dependency for the electrode signal

$$\frac{dC_E}{dt} = T_E(C - C_E) \tag{13}$$

result upon integration

$$C_E = C^* \left(1 - \frac{e^{-k_L a' t} - k_L a' T_E\, e^{-t/T_E}}{1 - k_L a' T_E}\right) \tag{14}$$

For low viscosity media (without CMC) the k_La' values were evaluated by fitting Eq. 14 to the experimentally observed electrode signal. For measurements in CMC solutions the time dependency of the electrode signal could be neglected and k_La' was determined from

$$ln(C^* - C_E) = k_L a' t + \text{constant} \tag{15}$$

The results of an exact treatment considering a second-order time dependency agreed within the experimental error. From the k_La' values the volumetric mass transfer coefficients with respect to dispersion volume were calculated from

$$k_L a = k_L a' \epsilon_L \tag{16}$$

When a surfactant was added, the influence of the stationary holdup of very small bubbles was incorporated into the mass balance according to the considerations of Heijnen et al. (1980). Because of the large surface to diameter ratio of these bubbles (d_B < 1 mm), they were assumed to be in equilibrium with the liquid phase.

$$C_{G,vs} = \frac{H}{RT} C \tag{17}$$

At the start of aeration, very small bubbles consist of nitrogen and then they steadily take up some of the oxygen transferred to the liquid phase. Already a small holdup of very small bubbles $\epsilon_{G,vs}$ retards the saturation process considerably by increasing the absorption capacity. At 298 K the equilibrium oxygen concentration in the gas is about 32 times higher than the liquid-phase concentration. The liquid-phase oxygen balance is

$$\frac{dC}{dt} + \frac{\epsilon_{G,vs}}{\epsilon_L}\frac{dC_{G,vs}}{dt} = k_L a'(C^* - C) \tag{18}$$

By introduction of Eq. 17 it follows

$$\frac{dC}{dt} = \frac{k_L a'}{\left(1 + \dfrac{\epsilon_{G,vs} H}{\epsilon_L RT}\right)}(C^* - C) \tag{19}$$

Neglecting the electrode time constant ($C_E = C$) integration results

$$ln(C^* - C_E) = \frac{k_L a'}{\left(1 + \dfrac{\epsilon_{G,vs} H}{\epsilon_L RT}\right)}(C^* - C) \tag{20}$$

The correction with respect to Eq. 15 required the knowledge of very small bubble holdup $\epsilon_{G,vs}$ from dynamic gas disengagement experiments.

For calculation of interfacial areas from the gas-phase conversions measured in the sulfite oxidation runs, the gas phase was assumed to be in plug flow. Dispersion of the gas phase was not critical because of the small gas-phase conversions encountered (<10% for all CMC/sulfite runs).

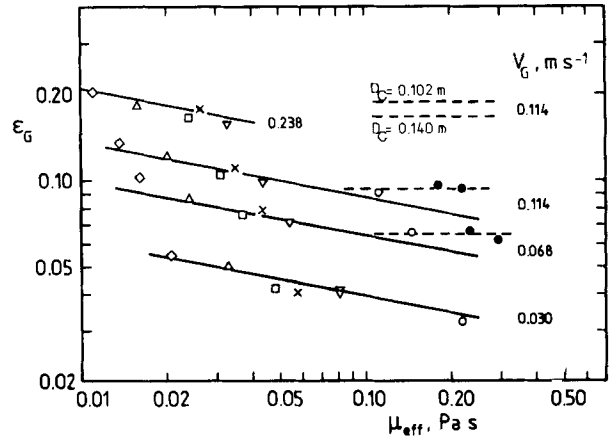

Figure 2. Gas holdup dependence on liquid-phase viscosity. (--- Churn-turbulent Flow Regime) (• • • • Slug Flow Regime) Solid Symbols for Solutions 6 & 7, ◇: Solution 1, △: Solution 2, □: Solution 3, ▽ Solution 4, ○: Solution 5 as in Table 1 for CMC Solutions.

For the interfacial area determination the condition

$$3 < Ha = \left(\frac{2k_2 D_L C^*}{3k_L{}^2}\right)^{0.5} \ll 1 + \frac{D_B C_{BO}}{2D_L C^*} \tag{21}$$

was fulfilled. This condition assured that the sulfite oxidation reaction in the bubble column occurred in the fast reaction regime and that the reaction was not an instantaneous reaction. The specific interfacial areas were calculated from the equation given by Schumpe and Deckwer (1982).

$$(1 - X_0)[f(X_1) - f(X_0)] = \frac{2aK_2P_T^{0.5}LRT[(1+\alpha)^{2.5} - 1]}{V_{GO}\quad 5(1+\alpha)\alpha} \tag{22}$$

where

$$f(X) = \frac{2 - 3X}{\sqrt{X(1-X)}} - \frac{3}{2} ln \frac{1 + \sqrt{X}}{1 - \sqrt{X}}$$

$$p = P_T(1 + \alpha(1 - z))$$

$$\alpha = L\rho_{LG}(1 - \epsilon_G)/P_T$$

RESULTS AND DISCUSSION

Gas Holdups and Flow Regimes

Large irregular-shaped bubbles move with high rise velocity in the presence of small bubbles for the churn-turbulent flow regime which occurs for large-diameter columns at high gas flow rates. In small-diameter columns, at high gas flow rates and high liquid viscosity, large bubbles are stabilized by the column wall leading to the formation of bubble slugs. In CMC solutions for the present column (D_C = 0.305 m) churn-turbulent flow prevailed up to a viscosity of about 0.1 Pa·s. For a smaller column of 0.14-m diameter, Schumpe and Deckwer (1982) observed the formation of gas slugs at viscosities of 0.02–0.03 Pa·s. In this work very few measurements were carried out in the slug flow regime, since the glass column vibrated vigorously.

In Figure 2 the relative gas holdups for four different gas velocities are plotted against the effective viscosity on a log-log scale. In the churn-turbulent flow regime the gas holdup decreased with increasing viscosity (solid lines). This agrees with the observations of Schumpe and Deckwer (1982) who also observed higher ϵ_G values in small-diameter columns. For a gas velocity of 0.114 m·s^{-1} the predictions of Eqs. 6 and 7 suggested by Schumpe and Deckwer (1982) for slug flow in columns of 0.102-m and 0.14-m diameter, respectively, are shown in Figure 2. The present holdup results in slug flow conditions are much smaller and indicate an even slightly higher diameter dependency than suggested by Eq. 8 (Godbole et al., 1982).

For CMC solutions the measured holdups in churn-turbulent flow are correlated by

$$\epsilon_G = 0.207\, V_G^{0.60}\, \mu_{eff}^{-0.19} \qquad \begin{matrix} ms^{-1} & Pa{\cdot}s \end{matrix} \tag{23}$$

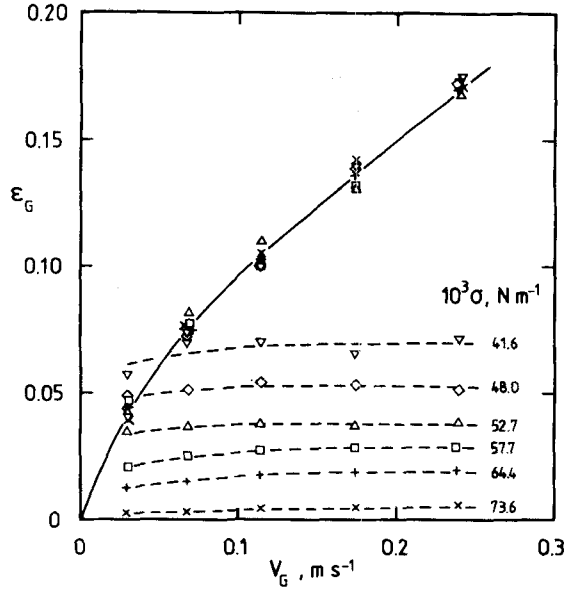

Figure 3. Dynamic gas disengagement data on effect of surface tension on gas holdup due to large bubbles (—) and small bubbles (----).

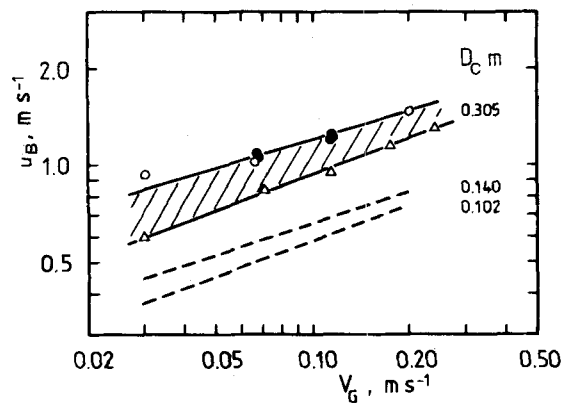

Figure 4. Effect of column diameter on the mean bubble rise velocity in CMC solutions.

with a mean deviation of ±4%. For CMC/salt solutions gas holdups can also be fitted against the group $(V_G^{0.60}\mu_{eff}^{-0.19})$ with a mean deviation of ±4%. The constant factor for CMC/salt solutions is 23% higher than the one for pure solutions.

$$\epsilon_G = 0.255 V_G^{0.60}\mu_{eff}^{-0.19} \qquad (24)$$

For CMC/salt solutions, only at the highest viscosity, gas slug formation seemed to take place near the top of the dispersion. The salt content of 0.8 mol·L^{-1} retarded the flow transition from 0.1 Pa·s in pure CMC solutions to about 0.2 Pa·s. At the point of transition, the gas holdups in CMC/salt solutions were similar to those observed for slug flow in pure CMC solutions at the same viscosity. Schumpe and Deckwer (1982) also reported the same gas holdups in CMC and CMC/salt solutions in the slug flow regime.

The effect of surfactant (Triton X-114) addition on the gas holdup structure was investigated at six different concentrations (below the critical micell concentration). The dynamic gas disengagement data (Figure 3) clearly show that the holdup of large bubbles was not affected by the surfactant. With increasing Triton concentration, the holdup due to very small bubbles ($d_B < 1$ mm) strongly increased. The holdup due to very small bubbles was negligible for pure CMC solutions but it amounted to 50–100% of the large-bubble holdup at the highest applied surfactant concentrations. Surprisingly, $\epsilon_{G,vs}$ hardly depends on the gas velocity. No correlation for the effect of Triton concentration or surface tension can be suggested.

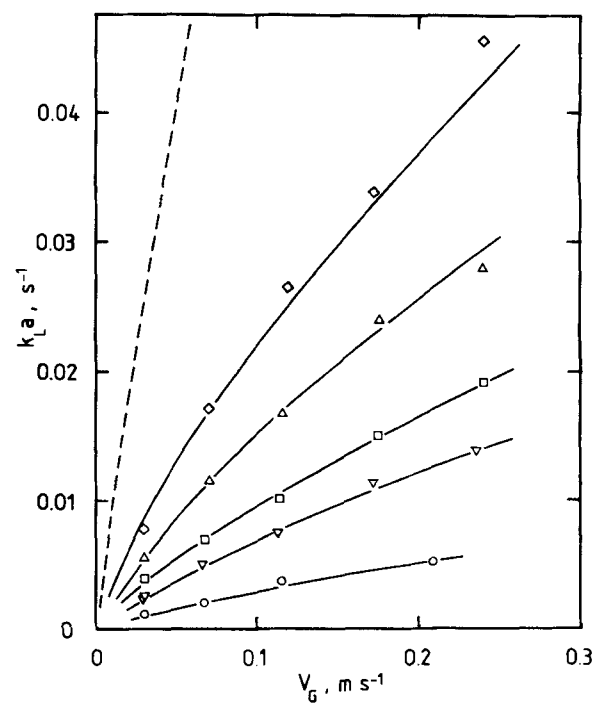

Figure 5. Volumetric mass transfer coefficient in CMC-solutions (---- water predicted by Eq. 26 (Shah et al., 1982). ○: Solution 5, ▽: Solution 4, □: Solution 3, △: Solution 2, ◇: Solution 1 as in Table 1 for pure CMC Solutions

In Figure 4 mean bubble rise velocities

$$U_B = V_G/\epsilon_G \qquad (25)$$

in CMC solutions are compared to determine the effect of column diameter. The values reported by Schumpe and Deckwer (1982) for gas slugs in columns of 0.102- and 0.14-m diameter (dotted lines) are independent of viscosity. For 0.305-m diameter column the mean bubble rise velocities were higher and increased with increasing viscosity. In the slug flow regime, bubble rise velocities reached an upper limit about twice those for the smaller diameters.

Volumetric Mass Transfer Coefficients

Volumetric mass transfer coefficients were determined by dynamic physical absorption in water and sodium sulfate solution. The k_La values for tap water agree fairly well with a correlation suggested by Shah et al. (1982):

$$k_La = 0.467\ V_G^{0.82} \qquad (26)$$
$$s^{-1} \qquad ms^{-1}$$

Equation 26 is based on k_La data obtained by the stationary method at gas velocities not exceeding 0.1 ms^{-1}. Thus, k_La data measured using dynamic and stationary methods are in agreement (±7%). In the sodium sulfate solution much higher values were obtained because of the presence of electrolytes.

In CMC solutions only the dynamic method was used. The sodium sulfate used in CMC/Sulfate solutions was prepared by complete oxidation of sodium sulfite solutions in order to maintain compatability to the interfacial area determinations.

Volumetric Mass Transfer Coefficients in CMC Solutions

Figure 5 shows the volumetric mass transfer coefficients determined in CMC solutions of five different concentrations at gas velocities up to 0.24 ms^{-1} along with the k_La values for water (as predicted by Eq. 26). Figure 6 gives the results for CMC/sodium sulfate solutions. In both figures a strong dependency on the CMC concentration can be seen.

Predicted mass transfer coefficients using correlation of Deckwer

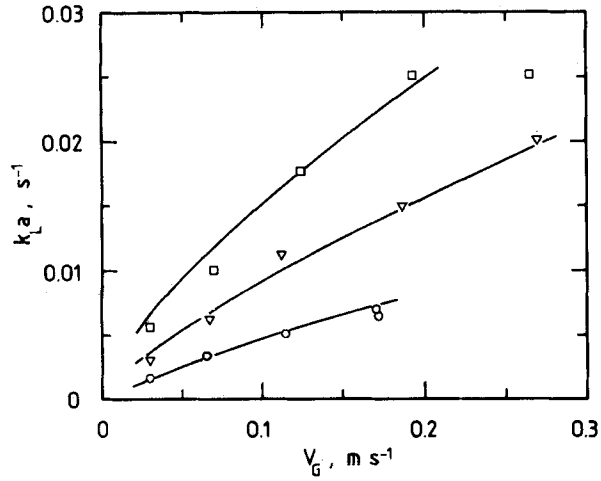

Figure 6. Volumetric mass transfer coefficients in CMC/sodium sulfate solutions. O: Solution 3; ▽: Solution 2, □: Solution 1 as in Table 1 for CMC/Sodium Sulfate Solution

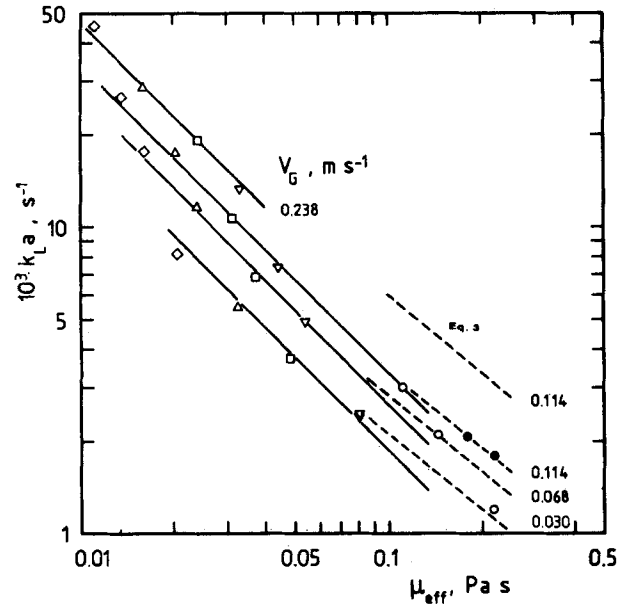

Figure 7. Log-log plot of liquid viscosity and volumetric mass transfer coefficients for CMC solutions in the heterogeneous flow regime (—) and in slug flow regime (---) (open symbols (heterogeneous flow regime)) and (solid symbols (slug flow regime)). Open symbols same as Figure 5.

et al. (1982) (Eq. 3) were higher by 20–70%. The correlation (Eqs. 1 and 2) of Nakanoh and Yoshida (1980) who used the same experimental procedure predicted even higher values. However, some extrapolation to higher viscosities is involved in the comparison. A strong dependency of the volumetric mass transfer coefficients on column diameter may be concluded. This corresponds to the strong decrease in gas holdup. The increase of k_La' with increasing column diameter predicted by Eq. 2 is unrealistic.

A regression analysis of the volumetric mass transfer coefficients measured at churn-turbulent flow results in:

$$k_La = 8.35 \times 10^{-4}\ V_G^{0.44}\ \mu_{eff}^{-1.01} \qquad (27)$$
$$(s^{-1}) \qquad (ms^{-1})\ (Pa{\cdot}s)$$

Equation 27 represents the experimental values with a mean deviation of only 3%.

The small number of data points for CMC/sulfate solutions did not seem to justify a separate correlation. Fitting against the same group ($V_G^{0.44}\ \mu_{eff}^{-1.01}$) the volumetric mass transfer coefficients in CMC/sulfate solution are correlated by:

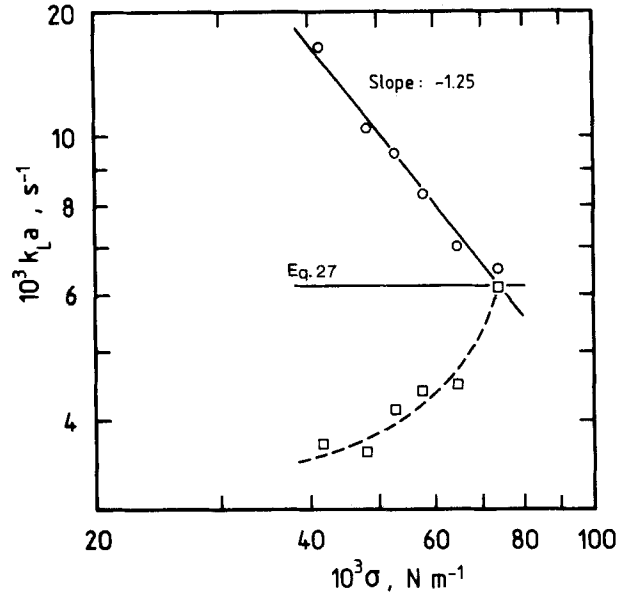

Figure 8. Volumetric mass transfer coefficients in CMC/surfactant solutions (O). (□: not corrected for very small bubbles).

$$k_La = 2.15 \times 10^{-3}\ V_G^{0.44}\ \mu_{eff}^{-1.01} \qquad (28)$$
$$(s^{-1}) \qquad (ms^{-1})\ (Pa{\cdot}s)$$

Obviously, addition of sodium sulfate strongly increased the volumetric mass transfer coefficient.

Volumetric mass transfer coefficients measured in CMC solutions are plotted against effective liquid viscosity on log-log scale (Figure 7). For churn-turbulent flow the data follow Eq. 27 (solid lines). The transition to slug flow seems to introduce a slightly weaker dependency on viscosity (dotted lines) like the one suggested by Deckwer et al. (1982) for this flow regime (Eq. 3). In this work the limited number of measurements did not allow firm conclusions for the slug flow regime.

Effect of Surfactant on Volumetric Mass Transfer Coefficients

To study the effect of surfactant, Triton X-114 (provided by Rohm and Haas) was added to a CMC solution in increasing concentrations. Figure 8 shows the volumetric mass transfer coefficients (circles) as a function of the equilibrium surface tension. The k_La value for the pure CMC solution is well represented by Eq. 27. With decreasing surface tension the volumetric mass transfer coefficients strongly increase:

$$k_La \alpha \sigma^{-1.25} \qquad (29)$$

However, the influence of the very small bubble holdup is rather strong: the values without correction even decreased with decreasing surface tension. Since surfactants are known to decrease the liquid-side mass transfer coefficients k_L (Kawase and Ulbrecht, 1982) the assumption of instant equilibrium between very small bubbles and liquid might not be valid. In addition, modeling did not consider the possible dynamic transfer between very small and large bubbles by coalescence and breakup. These effects would result in an overestimation of k_La; therefore, Eq. 29 is to be understood as an upper limit of the surface tension effect.

Specific Interfacial Areas

The specific interfacial areas were determined by the sulfite oxidation method. In the CMC/sulfite solutions the interfacial areas were much smaller than in the pure sodium sulfite solution and decreased with increasing CMC concentration. The dependency of interfacial area on liquid viscosity can be seen more clearly in the log-log plot given by Figure 9. For three gas velocities straight lines with slopes of about $-3/4$ are obtained (solid lines). For com-

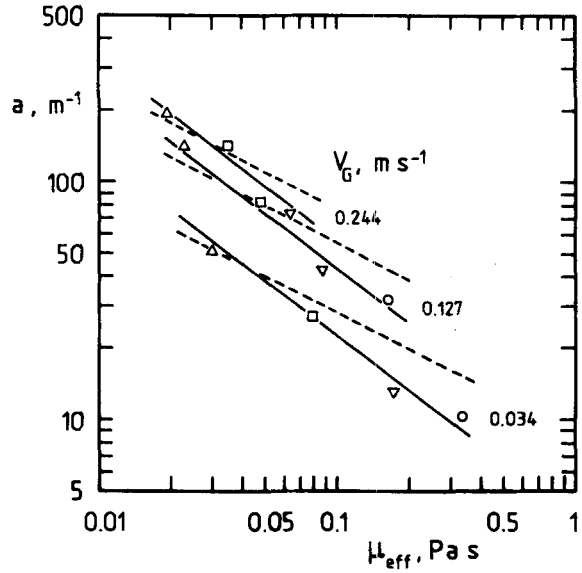

Figure 9. Dependence of specific gas-liquid interfacial area in CMC/sulfite solution on liquid-phase viscosity (--- Eq. 5 by Schumpe et al., 1982). △: Solution 1, □: Solution 2, ▽: Solution 3, ○: Solution 4 as in Table 1 for sodium-sulfite solutions.

parison the predictions of Eq. 5 suggested by Schumpe and Deckwer (1982) are also shown (dotted lines). The deviation is rather small at low viscosities although Eq. 5 is valid for slug flow in a 0.14-m diameter column. The present data for churn turbulent flow show a stronger dependency on effective viscosity:

$$a = 19.2\, V_G^{0.47} \quad \mu_{\text{eff}}^{-0.76} \qquad (30)$$
$$(\text{m}^{-1}) \quad (\text{ms}^{-1})\,(\text{Pa·s})$$

Equation 30 represents the experimental values with a mean deviation of ±10%.

Liquid-Side Mass Transfer Coefficients

The specific interfacial areas measured for CMC/sodium sulfite solutions in churn-turbulent flow regime are not representative of pure CMC solutions as is obvious from the salt effect on gas holdups and volumetric mass transfer coefficients. However, for the slug flow regime, Schumpe and Deckwer (1982) found no salt effect on ϵ_G and k_La.

Equation 30 for the interfacial area in churn-turbulent flow may be applied only to the volumetric mass transfer coefficients in CMC/sodium sulfate solutions. The resulting k_L values are shown in Figure 10. In accordance with Schumpe and Deckwer (1982), the dependency on the gas velocity is small but the present values are somewhat larger. No correlation or comparison with theoretical relations (Bhavraju et al., 1978) is given since the data are mean values for a broad and insufficiently known bubble-size distribution.

ACKNOWLEDGMENT

S. P. Godbole and A. Schumpe would like to thank Gulf Research and Development Co. for the financial support. Experimental work was also supported by Gulf Research and Development Co. and is gratefully acknowledged.

NOTATION

a = specific gas-liquid interfacial area per unit dispersion volume, m^{-1}
a' = specific gas-liquid interfacial area per unit clear liquid volume, m^{-1}

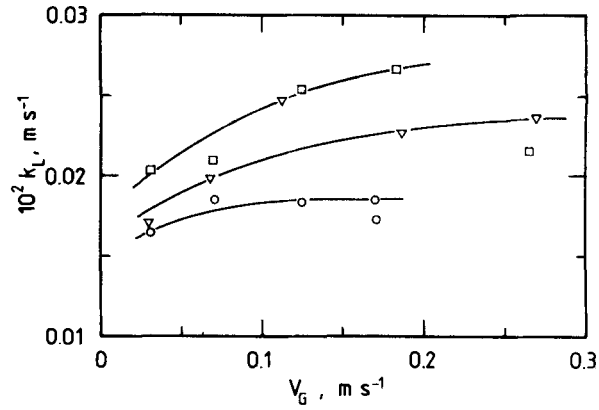

Figure 10. Liquid-phase mass transfer coefficients in CMC/sodium sulfate solutions. Symbols: ○: Solution 1, ▽: Solution 2, □: Solution 3 (See Table 1)

Bd = Bond number = $gD_C^2\rho_L/\sigma$, dimensionless
C = liquid-phase oxygen concentration, kmol/m^3
C^* = saturation concentration of oxygen, kmol/m^3
C_{BO} = bulk liquid-phase concentration of the liquid-phase reactant, kmol/m^3
C_E = electrode signal for corresponding, C, kmol/m^3
$C_{G,vs}$ = concentration of oxygen in very small bubbles in equilibrium with liquid, kmol/m^3
d_B = bubble size, mm
D_B = diffusion coefficient of the liquid-phase reactant, m^2/s
D_C = column diameter, m
De = Deborah number = $U_B\lambda/d_B$, dimensionless
D_L = diffusion coefficient of oxygen in the liquid, m^2/s
Fr = Froude number = $V_G/(gD_C)^{1/2}$, dimensionless
g = gravitational acceleration, m/s^2
Ga = Galilei number, = $g\rho_L^2D_c^3/\mu_L^2$, dimensionless
H = Henry's constant for O_2, $\text{Pa·m}^3/\text{kmol}$
Ha = Hatta number defined by Eq. 21, dimensionless
k = fluid consistency index, Pa·s^n
k_2 = reaction constant for a pseudosecond-order reaction, $\text{m}^3/\text{kmol·s}$
k_L = liquid-side mass transfer coefficient, m/s
K_2 = absorption reaction parameter defined by Eq. 9, $\text{kmol/m}^2\text{·s·Pa}^{3/2}$
L = dispersion height, m
n = flow-behavior index, dimensionless
P = pressure, Pa
P_T = pressure at the top of the column, Pa
R = gas constant, $\text{Pa·m}^3/\text{kmol·K}$
Sc = Schmidt number = $\mu_L/D_L\rho_L$, dimensionless
t = time, s
T = temperature, K
T_E = electrode time constant, s
U_B = average bubble rise velocity, m/s
V_G = superficial gas velocity, m/s
V_{Go} = V_G at the column inlet, m/s
X = O_2 mol fraction in gas, dimensionless
X_o = X at the inlet, dimensionless
X_1 = X at the outlet, dimensionless
z = axial distance, dimensionless

Greek Letters

α = defined below Eq. 22, dimensionless
γ = shear rate, L/s
γ_{eff} = effective shear rate (Eq. 4), L/s
ϵ_G = relative gas holdup, dimensionless
$\epsilon_{G,vs}$ = gas holdup due to small bubbles, dimensionless
ϵ_L = relative liquid holdup, dimensionless
λ = characteristic material time used in definition of De, s
μ = dynamic viscosity, Pa·s

μ_{eff} = effective dynamic liquid phase viscosity, Pa·s
ρ_L = liquid phase density, kg/m^3
σ = surface tension, N/m
Γ = shear stress, Pa

LITERATURE CITED

Akita, K., and F. Yoshida, "Gas Holdup and Volumetric Mass Transfer Coefficient in Bubble Columns," *Ind. Eng. Chem. Proc. Des. Dev.*, **12**, p. 76 (1973).

Bhavaraju, S. M., R. A. Mashelkar, and H. W. Blanch, "Bubble Motion and Mass Transfer in Non-Newtonian Fluids: Part I Single Bubble in Power law and Bingham Fluids," *AIChE J.*, **24**, p. 1063 (1978).

Buchholz, H., R. Buchholz, J. Lucke, and K. Schugerl, "Bubble Swarm Behavior and Gas Absorption in Non-Newtonian Fluids in Sparged Columns," *Chem. Eng. Sci.*, **33**, p. 1061 (1978).

Deckwer, W.D., K. Nguyen-tien, A. Schumpe, and Y. Serpemen, "Oxygen Mass Transfer into Aerated CMC Solutions in a Bubble Column," *Biotech. Bio. Eng.*, **24**, p. 461 (1982).

Franz, K., R. Buchholz, and K. Schugerl, "Comprehensive Study of the Gas Holdup and Bubble Size Distribution in Highly Viscous Liquids II: CMC Solutions," *Chem. Eng. Commun.*, **5**, p. 187 (1980).

Godbole, S. P., M. F. Honath, and Y. T. Shah, "Gas Holdup Structure in Highly Viscous Newtonian and Non-Newtonian Liquids in Bubble Columns," *Chem. Eng. Commun.*, **16**, p. 119 (1982).

Heijnen, J. J., K. van't Riet, and A. J. Wolthuis, "Dynamic k_La Measurement," *Biotech. Bioeng.*, **22**, p. 1945 (1980).

Henzler, H. J., "Begasen Hoherviskoser Flussigkeiten," *Chem. Ing. Tech.*, **52**, p. 8 (1980).

Kawase, Y., and J. J. Ulbrecht, "The Effect of Surfactant on Terminal Velocity of and Mass Transfer from a Fluid Sphere in a Non-Newtonian Fluid," *Can. J. Chem. Eng.*, **60**, p. 87 (1980).

Linek, V., and V. Vacek, "Chemical Engineering Use of Catalyzed Sulfite Oxidation Kinetics for the Determination of Mass Transfer Characteristics of Gas-Liquid Contactors," *Chem. Eng. Sci.*, **36**, p. 1747 (1981).

Nakanoh, M., and F. Yoshida, "Gas Absorption by Newtonian and Non-Newtonian Liquids in a Bubble Column," *Ind. Eng. Chem. Process Des. Dev.*, **19**, p. 190 (1980).

Nishikawa, M., H. Kato, and K. Hashimoto, "Heat Transfer in Aerated Tower Filled with Non-Newtonian Liquid," *Ind. Eng. Chem. Process Des. Dev.*, **16**, p. 133 (1977).

Onken, V., and W. Schalk, "Determination of Interfacial Area in Gas-Liquid Dispersions by Sulfite Oxidation," *Ger. Chem. Eng.*, **1**, p. 191 (1978).

Poggemann, R., "Stoffaustauschflache in Strahldusenreakton in Sbhaugigkeit von stoffichen EinfluBgrossen," Ph.D. Thesis, Universitat Dortmund (1982).

Schugerl, K., "Oxygen Transfer Into Highly Viscous Media," *Adv. Biochem. Eng.*, **19**, p. 71 (1981).

Schumpe, A., and W. D. Deckwer, "Analysis of Chemical Methods for Determination of Interfacial Areas in Gas-in-Liquid Dispersions with Nonuniform Bubble Sizes," *Chem. Eng. Sci.*, **35**, p. 2221 (1980a).

Schumpe, A., and W. D. Deckwer, "Vergleich der fotografischen und der Sulfit Oxidation Method zur Phasengrenzflachen Bestimmung in Blasensaulen," *Chem. Ing. Tech.*, **52**, p. 468 (1980b).

Schumpe, A., and W. D. Deckwer, "Gas Holdups, Specific Interfacial Areas, and Mass Transfer Coefficients in a Bubble Column," *Ind. Eng. Chem. Proc. Des. Dev.*, **21**, p. 706 (1982).

Schumpe, A., G. Quicker, and W. D. Deckwer, "Gas Solubilities in Microbial Culture Media," *Adv. Biochem. Eng.*, **24**, p. 1 (1982).

Shah, Y. T., B. G. Kelkar, S. P. Godbole, and W. D. Deckwer, "Design Parameters Estimations for Bubble Column Reactors," *AIChE J.*, **28**, p. 353 (1982).

Sriram, K., and R. Mann, "Dynamic Gas Disengagement: A New Technique for Assessing the Behavior of Bubble Columns," *Chem. Eng. Sci.*, **32**, p. 571 (1977).

Voigt, J., V. Hecht, and K. Schugerl, "Absorption of Oxygen in Countercurrent Multistage Bubble Columns II: Aqueous Solutions with High Viscosity," *Chem. Eng. Sci.*, **35**, p. 1325 (1980).

Wesselingh, J. A., and A. C. Van't Hoog, "Oxidation of Aqueous Sulfite Solutions: A Model Reaction For Measurements in Gas-Liquid Dispersions," *Trans. Inst. Chem. Engrs.*, **48**, p. T69 (1970).

Manuscript received January 7, 1983; revision received April 27, and accepted May 10, 1983.

Multivariable Computer Control of a Butane Hydrogenolysis Reactor

Part II: Design and On-Line Implementation of a Stochastic Controller Using an Identified Multivariate Noise Model

A multivariable stochastic controller is implemented on a pilot scale, plug flow, butane hydrogenolysis reactor. In the synthesis of the controller, a multivariate time series model of the process disturbances is used. The success of this controller is compared to a previous controller where the process disturbances are not directly modeled.

ARTHUR JUTAN and J. D. WRIGHT

Xerox Research Centre of Canada
Materials Processing Laboratory
Mississauga, Ontario, Canada

J. F. MACGREGOR

McMaster University
Hamilton, Ontario, Canada

SCOPE

Multivariable computer control of a packed-bed pilot-plant reactor has been studied by Jutan et al. (1977). A stochastic state space control algorithm was developed and implemented on the reactor in those studies. Although the multivariate stochastic disturbances entering the process were identified, they were not used in the synthesis of an optimal controller designed to specifically compensate for these disturbances. Instead, the

Correspondence concerning this paper should be addressed to A. Jutan.